Sustainable Energy Technologies and Assessments 53 (2022) 102425

Contents lists available at ScienceDirect

Sustainable Energy Technologies and Assessments

journal homepage: www.elsevier.com/locate/seta

Original article

Off-grid SeaWater Reverse Osmosis (SWRO) desalination driven by hybrid tidal range/solar PV systems: Sensitivity analysis and criteria for preliminary design

Agustín M. Delgado-Torres [a,*], Lourdes García-Rodríguez [b]

[a] Departamento de Ingeniería Industrial, Escuela Superior de Ingeniería y Tecnología (ESIT), Universidad de La Laguna (ULL), 38200 La Laguna, Tenerife, Spain
[b] Departamento de Ingeniería Energética, Escuela Técnica Superior de Ingeniería (ETSI), Universidad de Sevilla, 41092 Sevilla, Spain

ARTICLE INFO

Keywords:
Tidal range plants
Desalination
Reverse osmosis
Hybrid tidal/photovoltaic systems
Solar desalination, design criteria

ABSTRACT

This paper deals with innovative renewable energy (RE) - powered seawater reverse osmosis (SWRO) plants based on tidal range/PhotoVoltaic (PV) systems as a hybrid technology with interesting prospects to promote the RE desalination at medium to large capacity ranges. Key features to enhance solar PV with tidal range energy are the good temporary complementarity of both options and the predictable water production pattern that the tidal range plant allows, along with ensuring water production at night. Once the basic sizing of a power plant referred to a 20 MW turbine is conducted, the sensitivity analysis of main performance parameters of the hybrid solar/tidal desalination system is carried out through yearly simulations. With this analysis, an extension of the knowledge about the performance of hybrid tidal/solar desalination is gained in such a way that three useful design criteria are derived from the results: i) total investment cost per unitary water production, ii) energy consumed in desalination to total energy production, and iii) energy non-useful for desalination. Recommended designs are provided under each of these three criteria for given yearly freshwater demand with SWRO plants of 3.5 and 4.8 kWh/m^3 of specific energy consumption. Results proves that off-grid SWRO desalination powered by hybrid tidal/PV systems in a favorable location achieves actual water production of one half of nominal production with adequate selection of design parameters. Recommended sizing of the energy generator for minimizing capital costs corresponds to 20 MW tidal/25–27 MWp PV per 12 MW of SWRO consumption. Additionally, in absence of realistic costs data, the recommended design criterion for the plant sizing relies on the ratio of energy used by the desalination plant to that produced by the hybrid tidal/PV generator. Results at an exemplary plant location show that 14.1 $\times$ 10^6 m^3/y of fresh water obtained with desalination consumption of 3.5 kWh/m^3 needs 2.0 MW tidal/26.9 MWp PV. This energy system would produce 10 $\times$ 10^6 m^3/y considering 4.8 kWh/m^3 of specific consumption.

Introduction

Ocean energy has been analysed for seawater desalination since the last century, especially wave-driven systems as those reported by Crear and Pritchard (1991) [1], Crear et al (1987) [2] and Douglas et al (1989) [3]. However, such systems have been scarcely implemented in comparison to solar or wind-driven technologies. A thorough review of the first pilot systems can be found in García-Rodríguez (2001) [4]. Recent related papers published mainly focus on wave and tidal current energies, according to the excellent review conducted by Bundschuh et al (2021) [5]. It is worth noting that dedicated designs have been proposed to improve energy efficiency of the desalination system namely, shaft coupling of a tidal current turbine to the seawater intake pump that exhibits interesting cost prospects [6], or the direct coupling of a wave energy converter to the high-pressure pump of a SeaWater Reverse Osmosis (SWRO) plant, such as the so-called Wave2O™ [7]. The only concept of direct coupling that has been extensively assessed consists in the shaft connection of a tidal current turbine with horizontal axis and the main pump of the SWRO system. Yang et al (2020)[8] studied the coupling with piston pumps. Greco and Jarquìn-Laguna (2018) [9] and Chen at al (2019)[10] reported on system modelling whereas Ling at al (2019) [11] and Zhao et al [12] focused on experimental research. On the contrary, recent literature surveys carried out by the authors - Delgado-Torres et al (2020) [13] and Delgado-Torres and García-Rodríguez [14] - show that few papers analyze the coupling of

* Corresponding author.
E-mail addresses: amdelga@ull.es (A.M. Delgado-Torres), mgarcia17@us.es (L. García-Rodríguez).

https://doi.org/10.1016/j.seta.2022.102425
Received 10 February 2022; Received in revised form 11 June 2022; Accepted 14 June 2022
Available online 20 June 2022

Nomenclature

A_{basin}	Total basin area, m^2
A_{sluice}	Total sluice gaste's area, m^2
D	Turbine diameter, m
$E_{e,useless}$	Yearly useless energy, J
$E_{e,surplus}$	Yearly surplus energy, J
$E_{e,useful}$	Yearly useful energy, J
$E_{e,total}$	Total energy output of the hybrid plant, J
f_g	Electricity grid frequency, Hz
G_p	Number of generator poles
G_{PV}	Incident solar irradiance on the plane of the photovoltaic array, W/m^2
H_{sea}	Tide level, m
H_{basin}	Basin level, m
H	Available head, m
H_{min}	Minimum generation head, m
H_{st}	Generation starting head, m
IC	Total investment cost of the hybrid desalination system, USD
Ic_{tidal}	Unitary investment cost of the tidal range power plant, USD/kW
Ic_{PV}	Unitary investment cost of the solar photovoltaic plant, USD/kW_p
Ic_{SWRO}	Unitary investment cost of the desalination plant, USD/(m^3/d)
lt	Lifetime of the desalination plant, years
Q_p	Output capacity of the desalination plant, m^3/h
$P_{e,PV}$	Electrical power output of the solar photovoltaic plant, W
$P_{e,SWRO}$	Electrical nominal power consumption of the desalination plant, W
$P_{e,tidal}$	Electrical power output of the tidal range power plant, W
$P_{tidal,rated}$	Power output rating of the tidal range power plant, W
$P_{e,total}$	Electrical power output of the hybrid tidal range/solar photovoltaic energy system, W
$P_{e,useless}$	Useless electrical power output, W
$P_{e,surplus}$	Surplus electrical power output, W
$P_{PV,peak}$	Peak power of the photovoltaic plant
V_p	Volume of fresh water produced over the lifetime of the desalination plant, m^3
$V_{p,annual}$	Annual volume of fresh water produced, m^3/y
τ	Power availability factor
τ_{tidal}	Power availability factor computed only with tidal plant power output
τ_{PV}	Power availability factor computed only with solar photovoltaic plant power output
$\tau_{PV/tidal}$	Power availability factor of the hybrid system
Δt	Time interval

Abbreviations

AC	Alternative current
DC	Direct current
IRENA	International Renewable Energy Association
LCOE	Levelised Cost Of Energy
NREL	National Renewable Energy Laboratory
RO	Reverse Osmosis
PV	PhotoVoltaic
RE	Renewable Energy
SAM	System Advisor Model
SEC	Specific Energy Consumption
SWRO	SeaWater Reverse Osmosis
US	United States
0D	Zero – Dimensional

conventional tidal range power plants to SWRO desalination to become a dual-purpose plant.Table 1..

Within this frame, this paper deals with the innovative SWRO desalination based on the tidal range/PhotoVoltaic (PV) hybridization proposed by the authors (Delgado-Torres et al, 2020) [13] – see Fig. 1 -. In that work, the interesting prospects of this technology to promote Renewable-Energy (RE) - powered desalination were justified although no studies on the tidal range/PV hybridization have been conducted before.

Table 1
Key papers for further development of tidal current-powered desalination.

Ocean energy	Topic addressed	Reference
Tidal current	Experimental assessment of a tidal turbine	[37]
Tidal current	Experimental assessment of a tidal turbine	[38]
Tidal current	Optimized design of tidal turbines (blade design)	[39]
Tidal current	Optimized design of tidal turbines (blade number)	[40]
Tidal current	Optimized design of tidal turbines (anti-cavitation)	[41]
Tidal current	Modelling of a floating stream turbine	[42]
Tidal current	Assessment of resources and prospect in Malasya	[43]
Tidal current	Exploitation of resources at Tg Tuan coast	[44]
Tidal current	Exploitation potential at Manukau Harbour, New Zealand	[45]
Tidal current	Exploitation in Indonesia	[46]
Tidal current/ wave	Feasibility study in Iran	[47]
Tidal current/ wave	Experimental assessment of interactions	[48]
Tidal current/ wave	Modelling of tidal turbine	[49]
Tidal current /wind	Techo-economic assessment	[50]
Tidal current	Modelling of tidal current-driven SWRO desalination	[51]

Main advantages of hybrid tidal/PV energy systems for driving medium to large off-grid desalination plants in comparison to PV-powered desalination are the following:

-Unforeseen days with nil water production are impossible since tidal range resources are fully predictable. This allows to prevent periods with lack of freshwater production by inexpensive water storage instead of energy storage.

-The tidal plant allows a predictable water production pattern over nights and daylight whereas solar PV plant powers the water production mostly on daily and seasonal peak water demands. This results in a significantly expanded time of operation of the desalination plant.

Those issues solve key problems which likely are, along with high capital costs, the essential barriers for developing medium to large scale desalination based on off-grid RE systems. Therefore, hybrid PV/tidal-driven desalination should be explored in spite of the high costs of tidal energy in comparison to competitive costs of PV energy currently achieved. Estimations of electricity cost of 0.28–0.55 USD/kWh corresponding to nominal power of the tidal range plant lower than 10 MW are reported by Li et al (2018) [15], suitable to power nominal desalination capacities up to $68.5x10^3$ m^3/d. Therefore, 0.28 USD/kWh could be a reasonable estimation for medium to large capacity desalination in a favorable location. Such a high cost is similar than that of PV technology in the recent past, since IRENA [16] reports a global LCOE of utility-scale of 0.381 USD/kWh in 2010, which goes down to 0.057 USD/kWh (weighted average) in 2020.

The modeling approach of the tidal range/solar PV application to SWRO desalination was presented by the authors [13]. One of the most

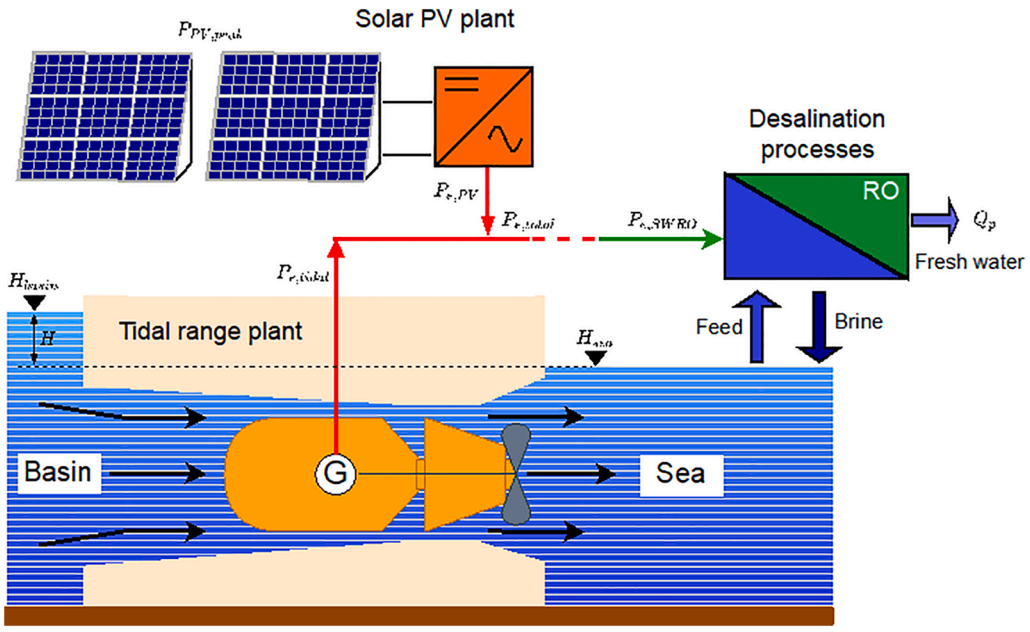

Fig. 1. Basic scheme of the hybrid solar PV/tidal range desalination system.

interesting findings about this energy combination was demonstrated with the quasi – dynamic simulation performed: the existence of days along the year with an excellent temporal complementarity between the tidal range and solar PV outputs. As an example, the freshwater production with the hybrid energy system would extend up to 2.4 times compared to any of both stand-alone plants. However, a comprehensive technology assessment was out of the scope. Therefore, main objectives of this paper are:

-the sensitivity analysis of different features of the energy systems as a function of the size of the solar PV generator and the nominal power consumption of the SWRO plant. A thorough optimization of the tidal plant operation such as that reported by Xue et al (2020) [17] is out of the aim of this paper.

-the preliminary design of a tidal range/solar PV desalination system referred to a 20 MW tidal turbine through different design criteria derived from the sensitivity analysis.

-the proposal of a design criteria for preliminary design purposes of tidal range/PV-driven desalination systems.

To this end, the same location (Broome, Australia) is selected to conduct this analysis due to its favorable tidal energy resources and because empirical tidal range data are available too. However, some qualitative results are considered not location-dependent. For further analyses, refer to WorldTides (2022) [18] for prediction of tides around the world and data of many tide stations and to Tidal Repository- Tidal Software (2022) [19] for dedicated software. Besides, different types of tidal range plants can be studied [20], being around 250 MW the largest production of a tidal range power plant that consists of 10 hydraulic turbines [21]. Therefore, a single turbine of this plant could drive a nominal desalination capacity up to about 170,000 m^3/d, being suitable to consider hydraulic turbines within a range of 8–25 MW. Additionally, hybrid energy systems minimize energy storage needs. As an exemplary technology, desalination based on combining wave, tidal current, solar and wind energies was proposed by Stuyfzand et al (2005) [22]. However, the conventional solution for discontinuous tidal energy is the energy storage [23], that could be based on compressed air [24], flywheels [25], supercapacitors [26], vanadium redox flow battery [25], hydrogen [27], hydropower [28] and undersea pumped storage [29]. Gude (2018) [30] presents an excellent general review on energy storage. Besides, Zakeri, and Syri [31] deal with the complementary aspect of life cycle cost analysis.

Future works of the authors on tidal range/PV-driven desalination will include other plant locations characterized in the literature as Mexico [32], Europe or Chile [33], linked-basin [34] tidal range plants in comparison to single-basin along with expanding desalination plant availability by means of including a wind power generator [35]. Concerning plant locations with limited tidal range resources, a key paper for considering the desalination projects based on exploiting existing resources is presented by Quaranta et al (2022) [36] dealing with very low tidal turbines designed for heads lower than 4.5 m. This technology could significantly develop medium to large capacity desalination by matching desalination demands and exploitable resources. However, policy barriers are expected in countries with no previous projects of tidal range power plants. This is a key issue that should be thoroughly studied.

On the other hand, desalination powered by tidal streams turbines is the recommended research topic on ocean-driven desalination for further development of small-medium capacity systems. The following table show some key papers, including technical advances and interesting potential locations along with studies on hybrid energy systems.

Finally, other complementary aspects to the system design rely on life cycle analyses, thermoeconomics and combining exergy and environmental point of views as the exemplary study reported by Shahbeig et al (2022) [52]. Also the net-zero exergoeconomic concept [53] should be investigated in sustainable desalination along with exergoenvironmental maps as those presented by Rahnama et al [54].

Methodology

To enable the general analysis of desalination plants driven by hybrid tidal/PV power generation, desalination capacity and peak power of the solar PV field are calculated considering a single tidal turbine with reasonable rated power. Therefore, the number of hydraulic turbines that will operate in parallel within the tidal plant can be easily selected as a function of the annual freshwater demand.

A favorable plant location allows to carry out an adequate analysis for preliminary design criteria of tidal/PV-driven desalination plants since it is based on qualitative results. However, sizing of main components significantly dependent on plant location and requires a case-by-case study.

Concerning the solar PV system, the PVWatts model available in the

System Advisor Model (SAM) developed by National Renewable Energy Laboratory (NREL) generates the energy output of the solar PV plant [55] per MWp installed. This is the solar input required by the dedicated software that has been developed to perform the following stages of the design analysis reported in this paper:

1. Selection of input parameters of the tidal range plant at a given location for the selected tidal turbine.
2. Calculation of power production throughout the year of tidal and PV generators along with combined production of the hybrid tidal/PV plant as a function of rated power (peak power). This parameter has been selected instead of the aperture area of the solar field in order to avoid any reference to specks of the solar panel.
3. Calculation of freshwater production corresponding to the available power output as a function of desalination plant capacity within a selected range of specific energy consumption.
4. Analysis of different criteria for the preliminary design of both, the solar PV field and the desalination plant corresponding to the rated power of a single tidal turbine.

Calculation procedure

Tidal range and PV plants

Fig. 2 illustrates the principle of operation of the tidal range plant considered. If the sea level is known (H_{sea}) the power output of the plant can be computed for fixed values of the total sluice gates area (A_{sluice}), total basin area (A_{basin}) along with starting head (H_{st}) and minimum head (H_{min}) of the tidal turbine. The detailed flowchart of the 0D modeling approach implemented can be consulted in Delgado-Torres et al (2020) [13]. Only one 20 MW tidal turbine is selected with the same specifications of that of the Swansea Bay Lagoon project, reported by Angeloudis and Falconer (2017) [56] (see Fig. 3). Therefore, a well - documented hydraulic turbine is modelled to cover a desalination capacity range from medium to large by operating one or several turbines in parallel. Power output and discharge flow curves computed with the hill – chart method are presented in Fig. 3. It describes operation at

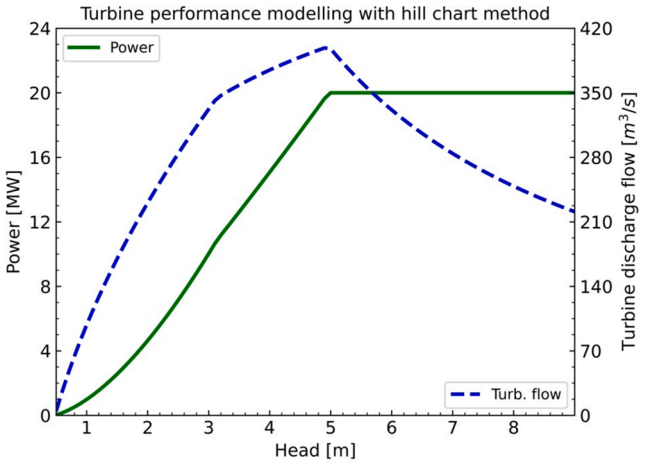

Fig. 3. Performance of the tidal turbine computed with the hill – chart method. Adapted from Delgado-Torres et al. (2020) [13] with permission.

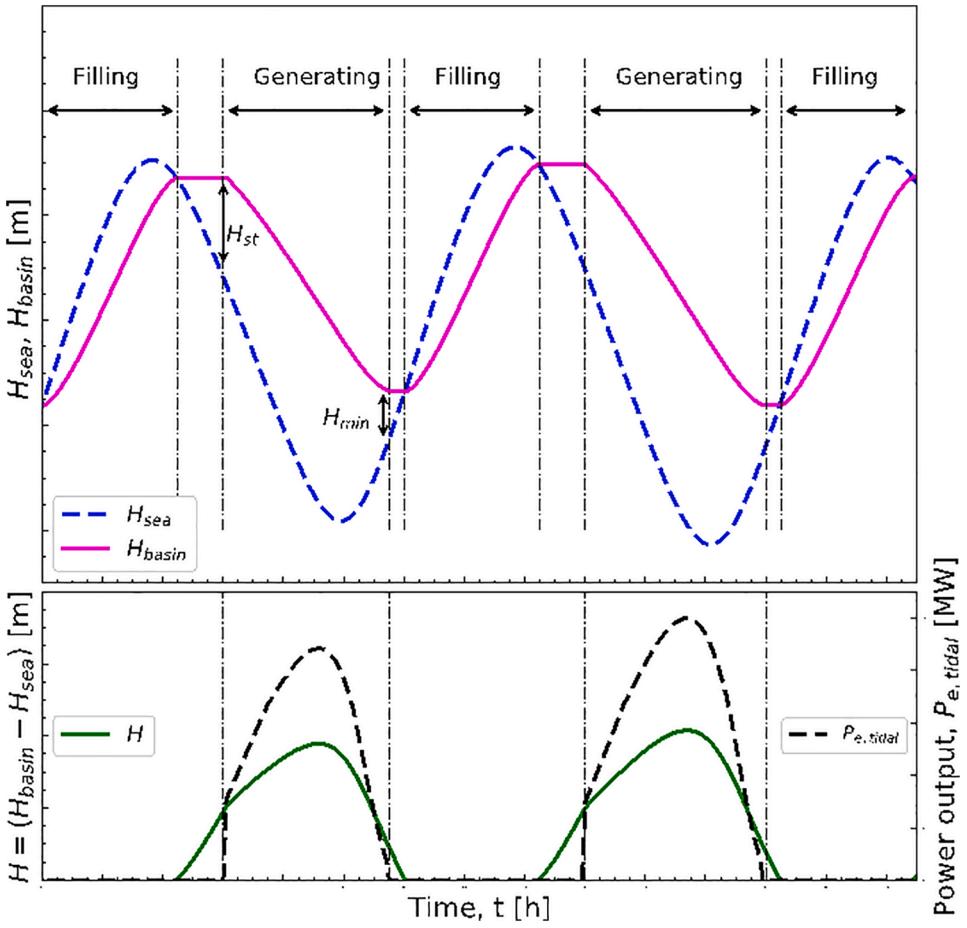

Fig. 2. Conceptual diagrams of operation modes and corresponding production in a tidal range power plant in ebb – mode. Adapted from Delgado-Torres et al. (2020) [13] with permission.

nominal power output if head (H) > 5 m as a result of the turbine regulation capabilities. Refer to Song et al (2020) [57] and Ewing et al (2020) [58] for additional details namely, fouling penalty and failure rates respectively.

Table 2 summarizes input parameters of the solar/tidal range system modelling, selected as described below. A basic sizing of a tidal range power plant was performed studying the influence of the basin and total sluice gate areas over the yearly energy output of the plant. For A_{basin} values between 2 and 5 km^2 there is a strong dependence of the yearly energy output on A_{sluice} for the range 100–200 m^2, but the effect of this parameter is much lower from 200 m^2 to 400 m^2. As a result, 3 km^2 and 200 m^2 were selected as reasonable respective areas for the basin and sluice gates since a detailed cost study to perform the best selection is out of the aim of this paper. Besides, the starting head of the tidal turbine has been individually analyzed to ensure that the value set in this study optimizes the annual energy output of the tidal range power plant for the given values of A_{basin} and A_{sluice}. The input parameters and their fixed values to run the model are also shown in Table 2. Hourly data of global irradiance were calculated from the meteorological data of the station at Broome airport obtained from [59].

Different time profiles that can be computed with the developed model are depicted in Fig. 4 on an exemplary seven-day period at Broome, Australia. In the first chart, the basin level goes up (filling mode) whenever the sea level is higher than the basin level, decreases if basin level is higher enough than sea level to allow the generating mode and remain unchanged over intermediate periods. The second chart depicts the available head ($H = H_{basin} - H_{sea}$) and the solar irradiance (G_{PV}), showing slight overlapping of turbine and PV field operation in the first days of the period.

Operation of the tidal/PV-driven desalination plant

Daily freshwater production from a given power generation profile depends on nominal capacity and Specific Energy Consumption (SEC) that ranges within 3.5–4.8 kWh/m^3 according to values reported for several desalination plants in Australia [60]. As conventional industrial plants, the SWRO system only operates at full capacity. Thus, a fixed nominal SEC is considered in the analysis performed. Quantitative results obtained in this paper are referred to 20 MW of tidal range power installed. Therefore, higher freshwater demands will be easily studied by means of parallel operation of several tidal turbines comprising the full tidal range plant with associated areas of basin and sluice gates along with corresponding peak power of the PV field and desalination production per each tidal turbine.

Table 2
Input parameters of the energy system modelling namely, tidal turbine specifications, main tidal power plant parameters, solar resource information and solar PV plant data.

Tidal turbine specifications	
Turbine model	Same as considered in Swansea bay Lagoon project [56]
Turbine capacity	20 MW
Generator poles, G_p	97
Turbine diameter, D	7.35 m
Electricity grid frequency, f_g	50 Hz
Turbine speed	61.9 rpm
Tidal system information	
Basin area, A_{basin}	3 km^2
Sluice area, A_{sluice}	200 m^2
Starting head, H_{st}	2 m
Minimum head, H_{min}	1 m
Solar resource information	
Annual global horizontal irradiation	2292 kWh/m^2
Annual direct normal irradiation	2544 kWh/m^2
Annual diffuse horizontal irradiation	554.8 kWh/m^2
Solar PV plant information	
Module type	Standard (crystalline Silicon)
Approximate Nominal Efficiency	17%
Module cover	Glass
Temperature coefficient	−0.47%/°C
DC to AC ratio	1.2
Inverter efficiency	96%
Array type and tilt	Fixed open rack, 18°
Azimuth	0° (North oriented)
Total system losses	14.08%

Two examples selected in this section show how the values of nominal power consumption of the desalination plant and the size of the solar PV generator (expressed by means of its peak power value, $P_{PV,peak}$) can affect the production period of water and, definitively, its annual quantity and temporal availability. For this reason, a sensitivity analysis should be performed to understand the performance of the hybrid desalination plant and derive design criteria for off-grid desalination plants.

An example of low tidal/solar overlapping corresponding to the summer of Broome in a spring tide period is shown in Fig. 5 where, as expected, the tidal power plant reaches its maximum power output (20 MW). The complementarity of the tidal and solar outputs is observed since the solar PV production is centered between the two semidiurnal tides (see the case of 24 December). However, the production period of the SWRO plant - and hence the freshwater production - strongly depends on the size of the solar PV generator. In this example the operating time of the SWRO plant at full load from 24th to 26th December would be 27.9 h with a 15 MW$_p$ generator and 47.1 h with the 30 MW$_p$ one.

The energy not usable for water production is also highlighted in the Fig. 5. Surplus power $P_{e,surplus}$ is given by the difference between the power output of the hybrid plant and the nominal power consumption of the SWRO plant. On the other hand, useless power corresponds to power production lower than this power consumption. The effect of the size of the solar PV generator on the useless energy is clearly observed as follows. For the 15 MW$_p$ generator, a significant portion of the solar PV energy produced around solar noon could not be consumed by the 15 MW SWRO plant. However, the energy produced would be consumed for desalination if a 30 MW$_p$ PV generator is considered. In this exemplary period, the useless energy would decrease from 299 MWh to 104 MWh when the solar PV generator grows form 15 MW$_p$ to 30 MW$_p$. The surplus energy exhibits the opposite trend, increasing from 130 MWh to 265 MWh.

To show the variety of situations that may arise throughout the year the case of a neap tide period without good complementarity between solar and tidal plants generation profiles is presented in Fig. 6. In this case the tidal power plant does not reach its maximum power output level at any time (20 MW) and the low temporal complementarity of both resources decreases with time. In fact, the maximum solar PV and tidal production are almost coincidental in time for January 11st. Consequently, there is a high penalty in the period of freshwater production since the energy produced by the tidal power plant in one of the two semidiurnal tides would not be consumed. In this case, growing the size of the solar PV plant implies an increasing of the freshwater production period but the energy output of the tidal plant would still not be consumed. Besides, the tidal range power generated after sunset becomes useless whatever the size of the PV generator. In addition, the surplus energy of the three days period is almost zero with the 15 MWp generator. Finally, when the $P_{PV,peak}$ grows up to 30 MW$_p$ the expected increase of the freshwater production is observed but also an increase in the surplus energy, mainly for the days with good radiation levels (January 10th and 11st). Next subsections describe the selected performance parameters of the SWRO desalination plant powered by the solar/tidal range power plant.

Power availability factor

The power availability factor (τ) was defined by the authors - Delgado-Torres et al (2020) [13] - to quantify the period of time during which the power demand of the reverse osmosis plant ($P_{e,SWRO}$) can be

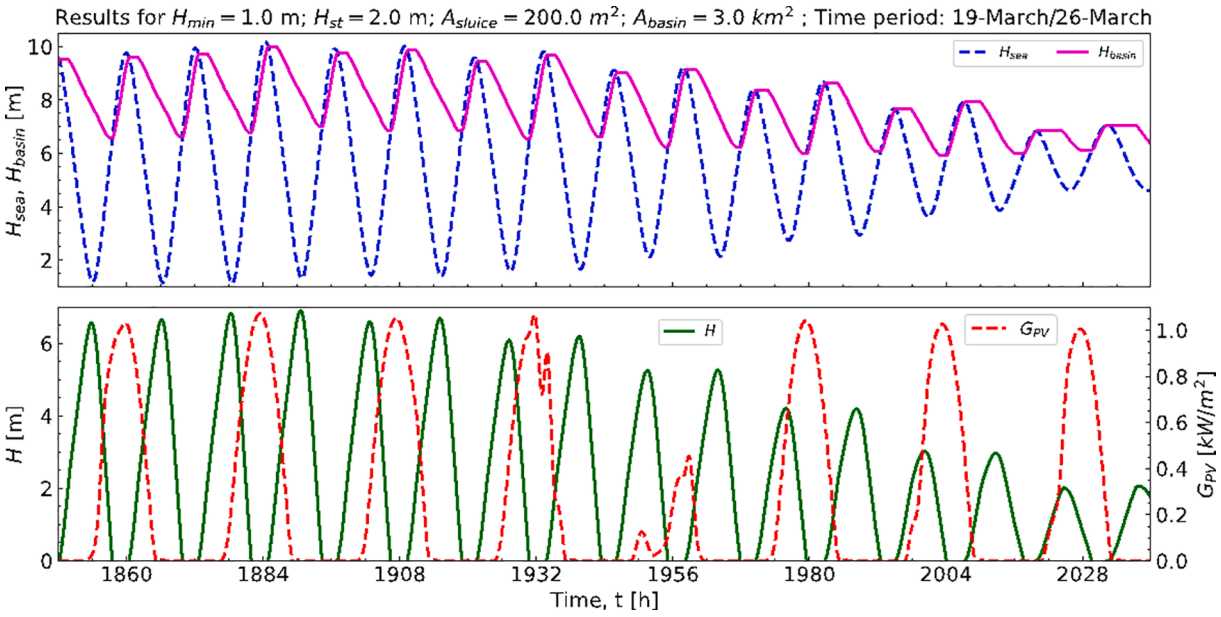

Fig. 4. Description of the hybrid tidal range/PV system operation in Broome, Australia.

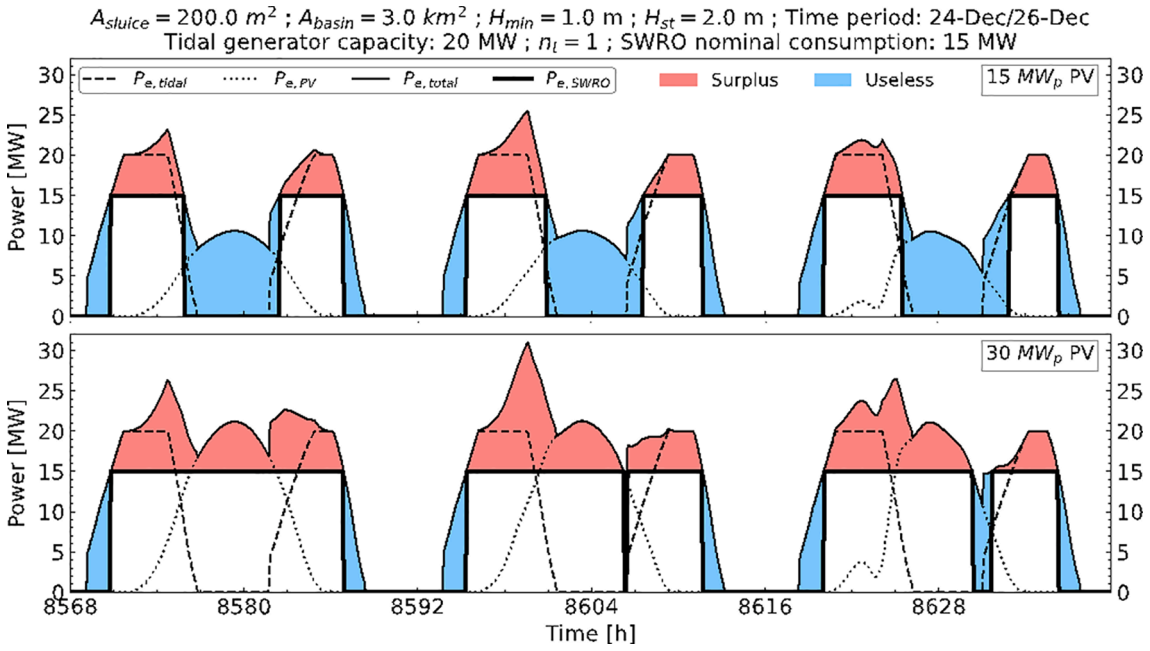

Fig. 5. Power output of the tidal, solar PV and hybrid plant and operation profile of the SWRO plant. Case: spring tide period in summer at Broome.

supplied by the power plant. In this study, the desalination plant operates only at full load, so this parameter corresponds to the capacity factor of the RE-powered desalination system and the availability of the desalination plant. Design decisions such us the potential use of energy backup would be based on this parameter, given by eq.1 in a yearly basis:

$$\tau_j(P_{e,SWRO}) = \frac{\Delta t_j\left(P_{e,j} \geq P_{e,SWRO}\right)[h]}{8760h} \quad (1)$$

where j = *tidal, PV* or *PV/tidal* for each of the three possibilities respectively: only the tidal plant in operation, only solar PV plant and hybrid solar PV/tidal plant. In the equation above Δt_{tidal}, Δt_{PV} and $\Delta t_{PV/tidal}$ are the total periods of time throughout the year, expressed in hours, during which the power output is equal to or greater than $P_{e,SWRO}$ with ezach option and $P_{e,PV/tidal} = P_{e,tidal} + P_{e,PV} = P_{e,total}$ in the hybrid case.

Surplus and useless energy

Useless energy output ($E_{e,useless}$) is relevant concerning decisions on installing batteries to expand the operation of the desalination plant. Moderate size of the batteries should be enough, and they would play an important role in the overall system avoiding effects of solar transient as much as permitting an early startup of the desalination plant. Final decisions on this regard correspond to the detailed cost analysis of the hybrid tidal/PV desalination system. Surplus energy ($E_{e,surplus}$) is a key parameter in adopting decisions in relation to the possible grid connection – if any – in order to sell the surplus energy. It should be noticed that surplus energy attributable to the solar PV system is

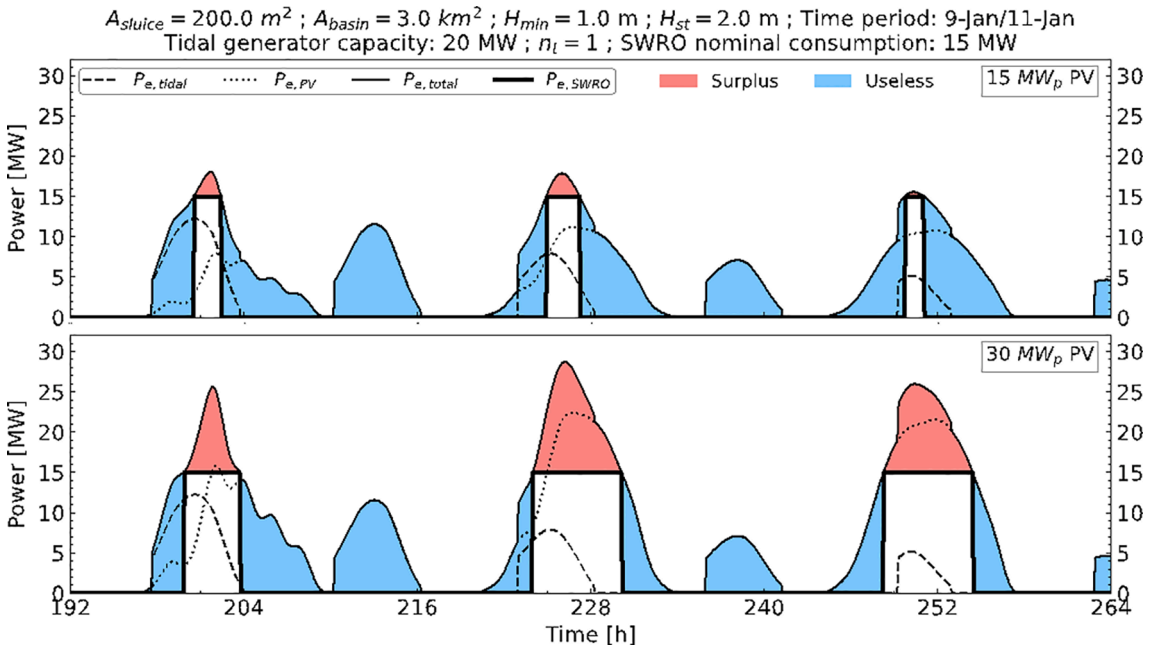

Fig. 6. Power output of the tidal, solar PV and hybrid plants and operation profile of the SWRO plant. No batteries are considered. Case: neap tide period in summer at Broome.

generated at demand peaks and the tidal plant production is fully predictable. In case of no batteries installed both, useless and surplus energy could be sold. If $E_{e,total}$ is the total energy output of the hybrid plant, the total energy not usable by the SWRO plant corresponds to the following equation:

$$(E_{e,surplus} + E_{e,useless}) = (E_{e,total} - \tau_{PV/tidal} \bullet 8760h \bullet P_{e,SWRO}) \quad (2)$$

Once the quasi – dynamic yearly simulation is performed the yearly useless energy in Equation (2) corresponds to eq.3:

$$E_{e,useless} = \int_0^{8760} P_{e,useless} \cdot dt \cong \sum_i P_{e,useless,i} \cdot \Delta t \quad (3)$$

where $P_{e,useless,i} = P_{e,total,i}$ if $P_{e,total,i} < P_{e,SWRO}$, otherwise $P_{e,useless,i} = 0\,MW$. Besides, the yearly surplus energy is given by eq.4:

$$E_{e,surplus} = \int_0^{8760} P_{e,surplus} \cdot dt \cong \sum_i P_{e,surplus,i} \cdot \Delta t \quad (4)$$

where $P_{e,surplus,i} = (P_{e,total,i} - P_{e,SWRO})$ if $P_{e,total,i} > P_{e,SWRO}$, otherwise $P_{e,surplus,i} = 0\,MW$.

Unitary investment cost

Because the high investment costs are a limiting factor in the development of medium- to large-capacity desalination systems, the prospect of a minimum investment cost per unit of desalinated water volume seems a reasonable criteria for final recommendations of design parameters of the hybrid desalination system in a specific location.

The total investment cost of the hybrid desalination system (*IC*) is expressed as the sum of the investment costs of the three main subsystems (tidal range, solar PV and SWRO desalination plants) computed from their respective unitary investment costs, Ic_{tidal}, Ic_{PV} and Ic_{SWRO} as follows (eq.5):

$$IC = Ic_{tidal} \cdot P_{tidal,rated} + Ic_{PV} \cdot P_{PV,peak} + Ic_{SWRO} \cdot Q_p \quad (5)$$

where Q_p is the SWRO desalination plant nominal capacity. The total volume of freshwater production over a lifetime *lt* is (eq.6):

$$V_p = lt \bullet \tau_{PV/tidal} \bullet 8760h/y \bullet Q_p \quad (6)$$

From eqs. 5–6, the specific unitary investment cost is calculated by means of eq.7:

$$\left(\frac{IC}{V_p}\right) = \left(Ic_{tidal} \cdot \frac{P_{tidal,rated}}{V_p} + Ic_{PV} \cdot \frac{P_{PV,peak}}{V_p} + Ic_{SWRO} \cdot \frac{P_{e,SWRO}}{SEC \cdot V_p}\right) \quad (7)$$

Operating assessment: Results and discussion

Some operating parameters are studied in this section to identify those that exhibit a maximum or minimum to become a potential parameter to optimize the preliminary design. Parameters analyzed comprise power availability factor, useless and surplus energy and unitary investment costs as described in the following subsections.

Analysis of power availability factor

The evolution of τ_{tidal} and τ_{PV} as a function of the nominal consumption of the SWRO plant is shown in Fig. 7, thus comparing tidal range/SWRO to PV/SWRO technologies referred to the rated power of the energy system and the nominal consumption of the SWRO plant. The τ_{tidal} exhibits an approximately linear decrease and it falls to zero when $P_{e,SWRO}$ is equal to the maximum capacity of the tidal turbine (20 MW). On the other hand, since τ_{PV} values are computed after a quasi-dynamic yearly simulation of the plant, this factor is null from $P_{e,SWRO}$ values below the peak power of the PV generator because peak conditions are achieved on a very low frequency throughout the year. For instance, $\tau_{PV} = 0\%$ for $P_{e,SWRO} = 12$ MW and$P_{e,SWRO} = 16$ MW when $P_{PV,peak} = 15$ MW and $P_{PV,peak} = 20$ MW respectively. The case of $P_{PV,peak} = 29$ MW would correspond to a solar PV plant with the same τ_{PV} value (7%) at the same maximum power level of the tidal range plant. These quantitative results of Fig. 7 are site - dependent through the solar and tidal resources but the qualitative result can be considered as general.

In addition, the performance of the SWRO desalination plant powered by the hybrid tidal range/solar system is analyzed by means of Fig. 8 as follows. The contour plot of $\tau_{PV/tidal}$ is shown in Fig. 8 overlapped with the color contour plot of τ_{PV}. Within the intervals of study, $\tau_{PV/tidal}$ may reach the value of 66% by selecting small desalination plant

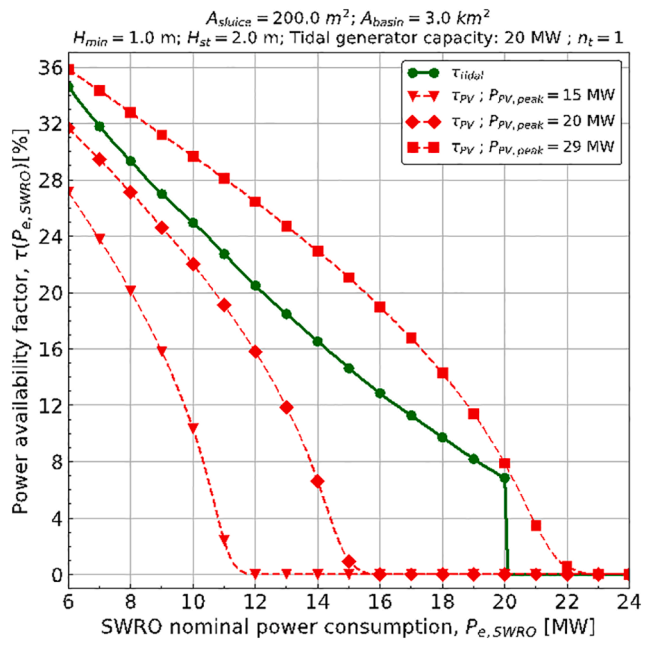

Fig. 7. Power availability factor of the 20 MW tidal range/SWRO plant and three different solar PV/SWRO plants as a function of $\mathbf{P_{e,SWRO}}$.

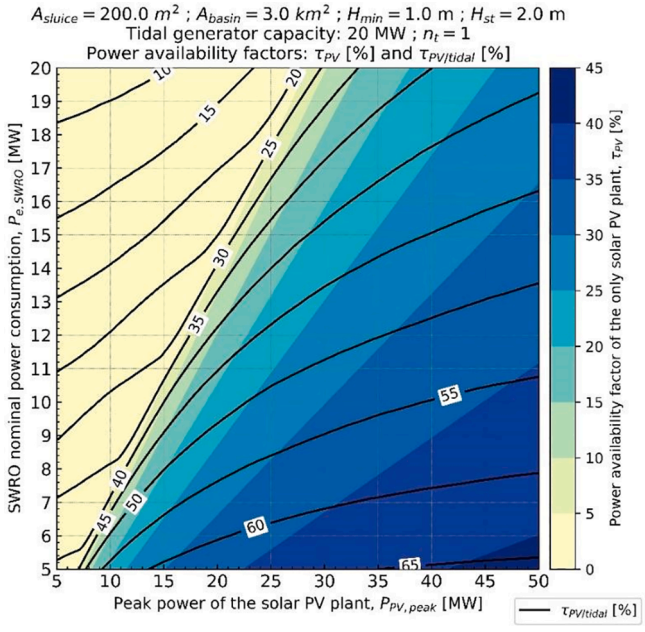

Fig. 8. Power availability factor of the hybrid and only solar PV powered SWRO plant.

and large PV generator. For any fixed value of $P_{e,SWRO}$ a narrow interval of $P_{PV,peak}$ values where a rapid growth of $\tau_{PV/tidal}$ occurs is observed. Moreover, a secondary - but also interesting - result is the asymptotic nature of $\tau_{PV/tidal}$ with respect to the size of the solar PV generator for $P_{PV,peak}$ values beyond the mentioned narrow interval.

The benefit of the solar PV/tidal combination can be also appreciated in Table 3. Some numerical values of τ_{PV} and $\tau_{PV/tidal}$ are given, including the values of $P_{PV,peak}$ that yield $\tau_{PV} = 1\%$. This means approximately the minimum peak power of the solar field that can drive the SWRO desalination plant. τ_{tidal} is also provided for each of the nominal SWRO consumption values. This factor grows along with the size of the SWRO plant. Regarding the improvement over the purely photovoltaic option, the hybridization leads to an effective use of the energy produced by the photovoltaic plant since values of $\tau_{PV/tidal}$ between 7.3% and 41% are possible in the region where $\tau_{PV} = 0$ – see first column of Table 3 -. Exemplary results for 10 MW of SWRO nominal consumption are given in the third row. As an additional result, τ_{PV} remains below 0.1% up to a value of the size of the PV generator of 12.4 MW for a nominal load of the SWRO of 10 MW and a power availability factor of 32%.

Therefore, the benefits of the hybrid energy system are clear. Indeed, a desalination plant with a nominal power consumption higher than the maximum capacity of the tidal range power plant and, thus, with $\tau_{tidal} = 0\%$ could be powered by the hybrid plant even with a solar PV generator which would yield $\tau_{PV} = 0\%$ too.

The rule of the direct sum $\tau_{PV/tidal} = \tau_{PV} + \tau_{tidal}$ is not fulfilled, being this aspect a good measure of the temporal complementarity of both solar PV and tidal range technologies. To quantify this complementarity the ratio of $\tau_{PV/tidal}$ to $(\tau_{PV} + \tau_{tidal})$ was computed (see Fig. 9). This ratio quantifies the advantages of the hybridization over the operation of the two subsystems independently. As can be observed, for a fixed nominal load of the SWRO plant there is a specific size of the solar PV plant that maximizes this ratio. This maximum will be characterized in the next

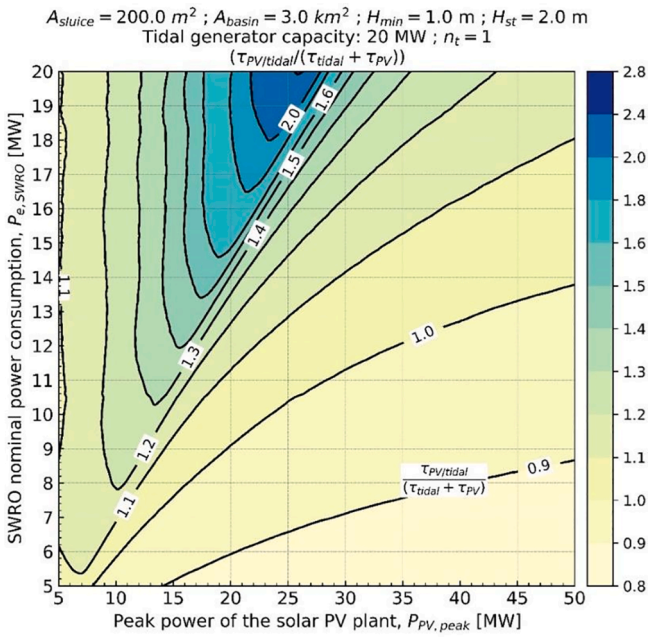

Fig. 9. Analysis of the benefits of hybrid energy system in SWRO desalination in terms of the ratio $\tau_{PV/tidal}$ to $\tau_{PV} + \tau_{tidal}$.

Table 3
Annual power availability factors. $A_{sluice} = 200\ m^2$, $A_{basin} = 3.0\ km^2$, $H_{min} = 1$ m and $H_{st} = 2$ m. Values in the table correspond to τ_{PV} [%]/$\tau_{PV/tidal}$ [%].

$P_{e,SWRO}$ [MW]	τ_{tidal}[%]	$P_{PV,peak}$[MW]						
		5	6.7	13.3	20	26.7	35	50
20	6.0	0.0/7.3	0.0/7.5	0.0/9.0	0.0/12.2	**1.0**/17.9	17.7/31.7	27.1/38.5
15	14.6	0.0/16.0	0.0/16.7	0.0/19.9	**1.0**/25.2	18.4/38.8	25.7/43.7	31.7/47.3
10	25.0	0.0/27.2	0.0/28.3	**1.0**/33.2	22.0/48.3	28.3/51.9	32.3/54.2	36.1/56.3
5	38.1	0.0/40.8	**1.0**/42.4	28.3/59.9	34.0/62.8	36.7/64.0	38.7/64.9	40.9/65.7

section. Finally, for low $P_{e,SWRO}$ and high $P_{PV,peak}$ there will be no advantage of the hybrid system.

Analysis of useless and surplus energy

The yearly values of surplus, useless and useful energy for desalination are depicted in Fig. 10. Since $P_{e,SWRO}$ is fixed, $E_{e,useful}$ exhibits the same dependence on $P_{PV,peak}$ as the power availability factor shown in Fig. 8. Therefore, a rapid increase is observed from $P_{PV,peak} = 19$ MW and this growth is continuous as the size of the generator rises, although the rate at which this happens gradually decreases for high values of the peak power. In Fig. 10, $E_{e,useful}$ grows from 31 GWh to 44 GWh when $P_{PV,peak}$ rises from 19 to 23 MW and from 59 GWh to 60 GWh if $P_{PV,peak}$ rises from 39 MW to 43 MW approximately. Since the total energy output of the hybrid plant grows linearly with the size of the solar PV generator, the trend of $E_{e,useful}$ gives rise to a maximum in the $E_{e,useful}$ to $E_{e,total}$ ratio, which implies the best relative use of the energy produced by the hybrid plant for desalination. This maximum exists within the entire interval of $P_{e,SWRO}$ selected for this study (see Fig. 11). Optimal values of ($E_{e,useful}/E_{e,total}$) between 39% and 55% can be attained with the 20 MW tidal hybrid plant for nominal consumptions of the SWRO plant between 5 MW and 20 MW. The absolute maximum of 54.8% is observed for $P_{e,SWRO} = 14.6$ MW when $P_{PV,peak} = 28.4$ MW.

Regarding the useless energy in Fig. 10 ($E_{e,useless}$), it grows until $P_{PV,peak}$ is slightly higher than the nominal value of power consumed by the desalination plant. This increase is due to the growth of the energy output of the solar generator as its size increases, but also because it is not capable of making a significant contribution to the energy useful for desalination. Above a certain value of $P_{PV,peak}$ (around 19 MW in Fig. 10), the photovoltaic plant starts its significant contribution to the energy useful for desalination thanks to its combination with the tidal range power plant. This implies a gradual reduction of the energy that cannot be consumed by the desalination plant (useless energy). The observed result in Fig. 10 for $P_{e,SWRO} = 15$ MW is found whatever the size of the SWRO plant.

Under a conventional operation mode of the SWRO plant the yearly non-useful energy output of the hybrid plant for seawater desalination would be the sum of ($E_{e,useless} + E_{e,surplus}$). This sum is dominated by the useless energy contribution in the low $P_{PV,peak}$ range and by the surplus energy contribution for high $P_{PV,peak}$ values (see Fig. 10). From the value of $P_{PV,peak}$ at which the solar PV plant increases its contribution to the desalination process, the opposite trends of $E_{e,useless}$ and $E_{e,surplus}$ yield a minimum in their sum (around $P_{PV,peak} = 25$ MW in the example). This result is found in the entire $P_{e,SWRO}$ interval of this study as it is shown in Fig. 12 where the existence of an absolute minimum of ($E_{e,useless} + E_{e,surplus}$) can be appreciated.

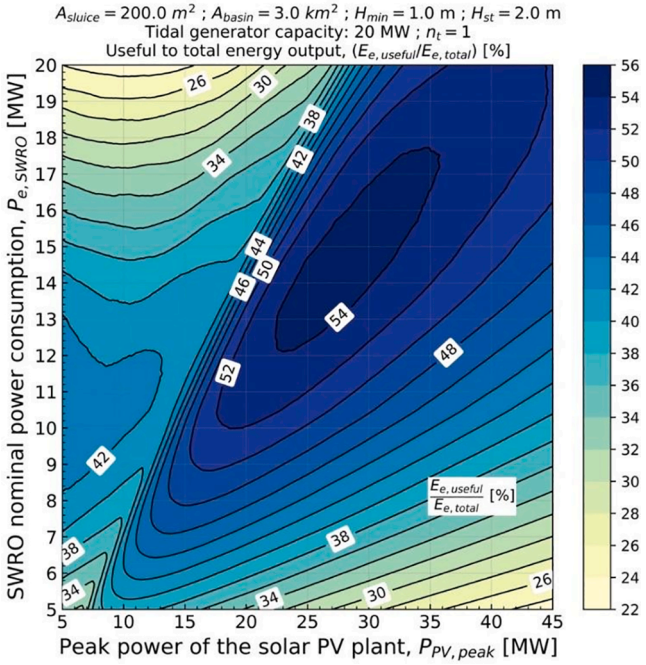

Fig. 11. Ratio $E_{e,useful}$ to $E_{e,total}$ within the range of $P_{e,SWRO}$ from 5 MW to 20 MW.

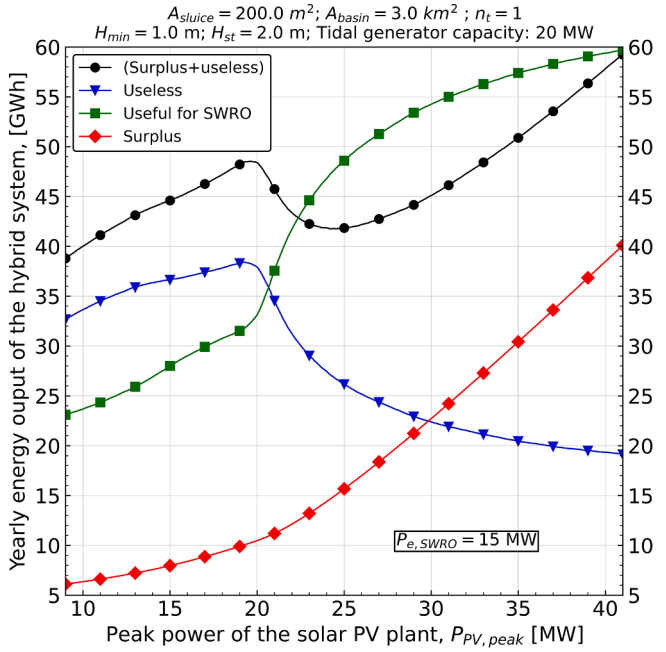

Fig. 10. Yearly surplus, useless and useful energy as a function of the size of solar PV plant for a fixed value of the SWRO nominal power consumption ($\mathbf{P_{e,SWRO}} = 15$ MW).

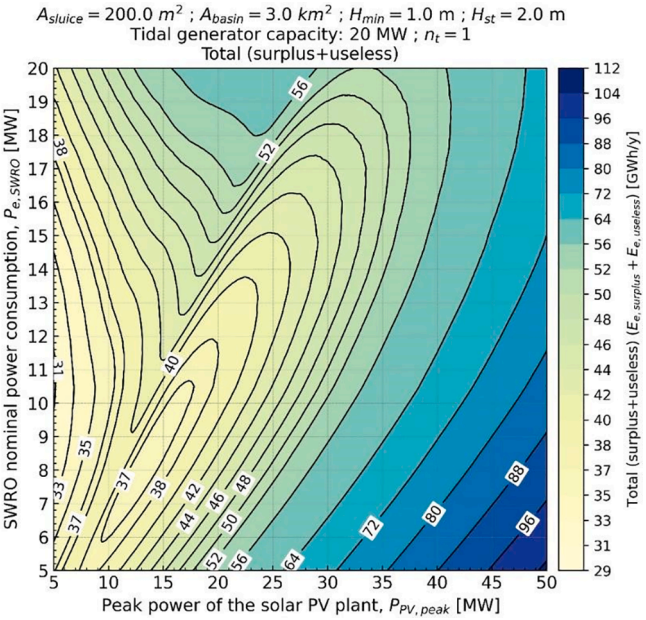

Fig. 12. Unused energy output (surplus + useless) energy output of the hybrid plant as a function of the size of the PV generator and the nominal power consumption of the RO desalination.

Analysis based on unitary investment cost

This section proposes a design criterion for the hybrid desalination plant based on simple economic input data without requiring a full set of economic and financial parameters of the plant scenario. The unitary investment cost estimation (IC/V_p) of the hybrid desalination plant is shown in Fig. 13 a) and b) as a function of the size of the PV generator along with the three different unitary costs associated with the tidal, solar PV and SWRO desalination. For utility-scale solar PV plants a value of 1061 USD/kW for Australia was assumed according to IRENA [16]. Besides that, an average of 500 USD/kW was considered for tidal range power plants considering the same source [61] in relation to projects planned in 2014. Both figures correspond to SWRO plants with the same nominal power consumption of 12 MW, but a SEC of 3.5 kWh/m^3 (nominal capacity of 82,286 m^3/d) in figure a) and a SEC of 4.8 kWh/m^3 (nominal capacity of 60,000 m^3/d) in figure b. The yearly volume of fresh water produced ($V_{p,annual}$, right y - axis) is also shown in the figure.

Since $V_{p,annual}$ is directly proportional to the power availability factor ($\tau_{PV/tidal}$), a continuous reduction of (IC_{tidal}/V_p) is observed because its investment cost is initially fixed when the nominal power of the tidal generator is set (20 MW). The situation is analogous in the case of (IC_{SWRO}/V_p). The greater use of the energy produced by the solar PV plant for desalination is evident in the significant decrease of the latter. However, the effect of $P_{PV,peak}$ on (IC_{PV}/V_p) is the opposite of the previous two, in general, which is explained by the increase of the surplus energy with the size of the PV generator. This growing tendency of (IC_{PV}/V_p) produces the minimum in the unitary investment cost (IC/V_p). This optimal point corresponds to a value of $P_{PV,peak}$ that slightly depends on SEC - $P_{PV,peak}$ = 29.3 MW and 27.9 MW for SEC = 3.5 kWh/m^3 and 4.8 kWh/m^3 respectively - with IC/V_p values of 0.61 USD/m^3 and 0.68 USD/m^3, also respectively. Additional interesting results are also observed in Fig. 13. Firstly, the rise in the contribution of the solar PV plant to the production of useful energy for desalination has a significant effect on the unit cost of the SWRO plant. Secondly, the contribution of the desalination plant to the total unitary investment cost is the highest of the three contributions and the contribution of the tidal plant is the lowest. To generalize the results of Fig. 13, the contour graph of IC/V_p is shown in Fig. 14 for the case of SEC = 3.5 kWh/m^3. As can be seen, the decrease already discussed of IC/V_p is present for any value of the nominal power consumption of the desalination plant. Analogous results

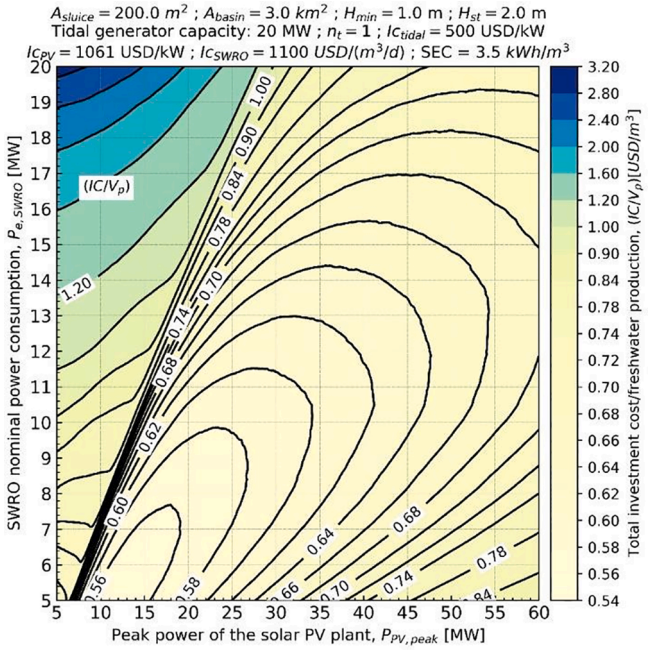

Fig. 14. Total unitary investment cost of the hybrid driven desalination plant - SEC = 3.5 kWh/m^3-.

are obtained for SEC = 4.8 kWh/m^3. Finally, Fig. 15 shows similar recommended sizing regardless the SEC and corresponding IC/V_p values.

Discussion on design criteria

The size of the solar PV generator at optimal values of ($E_{e,useless} + E_{e,surplus}$), ($E_{e,useful}/E_{e,total}$), ($IC/V_p$) and $\tau_{PV/tidal}/(\tau_{PV} + \tau_{tidal})$ as a function of the nominal power consumption of the SWRO plant is given in Fig. 16a, showing also the corresponding nominal capacity scale. Results were obtained for SEC of 3.5 kWh/m^3. The yearly freshwater production and the unitary investment cost are also depicted in the Fig. 16**b**. From the qualitative point of view, these results are independent of the SWRO

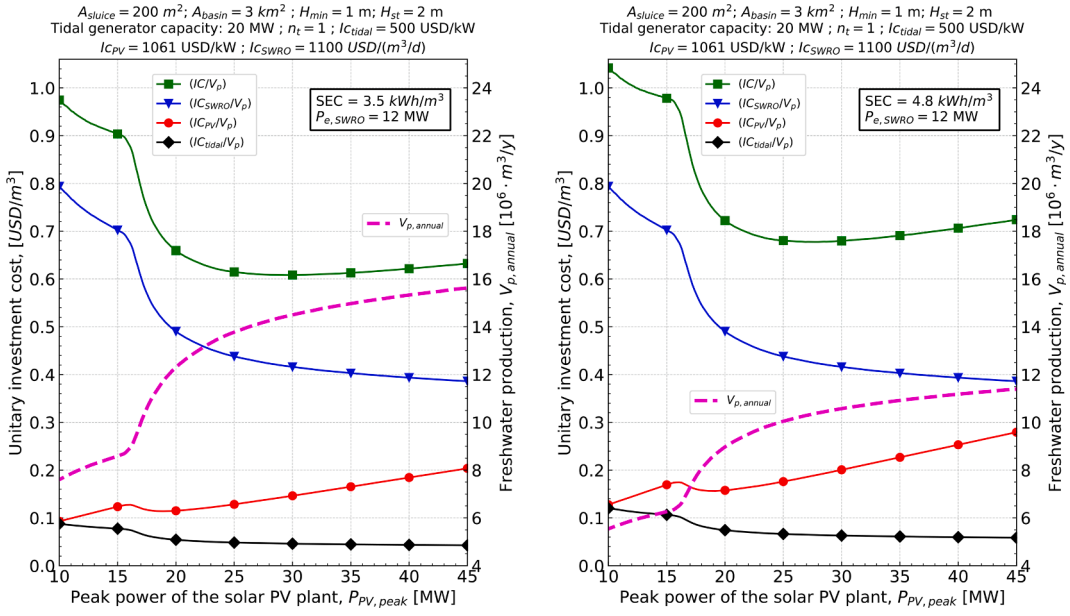

Fig. 13. Results for desalination power consumption of 12 MW: a) SEC = 3.5 kWh/m^3 and b) SEC = 4.8 kWh/m^3.

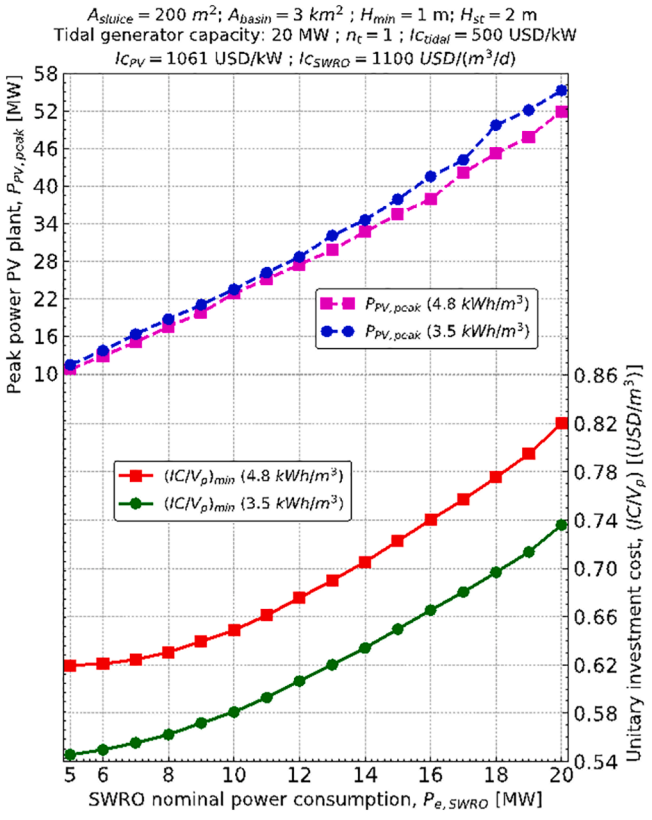

Fig. 15. Total unitary investment cost and recommended PV field within the range of SEC from 3.5 kWh/m^3 to 4.8 kWh/m^3.

plant's efficiency since same trends are observed for a SEC of 4.8 kWh/m^3.

As a general comparative trend among the four design criteria for a fixed desalination capacity - and hence investment cost of the desalination plant -, the larger the size of the solar PV generator, the lower the unitary investment cost. This result is due to the higher number of operating hours of the desalination plant (higher $\tau_{PV/tidal}$, see Fig. 8) and higher freshwater production.

Regarding each criterion, the maximum-time complementarity criterion implies, by far, the highest unit investment cost, which justifies that this criterion should be discarded. Moreover, for the same SWRO plant's capacity a maximum use of its total energy output would produce more fresh water than the plant designed under the two other operating criteria and achieving unit capital cost close to the minimum possible. If the minimization of the non-useful energy were the goal a higher unitary investment cost is observed.

For a given nominal capacity of the SWRO plant, minimizing IC/V_p leads to higher PV field size than those corresponding to other design criteria due to the dominant contribution of the desalination cost in comparison to the PV field. This behavior increases with the nominal capacity of the desalination plant, which is attributable to the low power availability achieved as the nominal desalination consumption increases, thus resulting in long periods with nil water production. However, dedicated designs could be adopted in order to fit the power curve demand to the power outputs such as those developed for wind or solar PV-driven desalination, reported by Subiela et al (2020) [62] who also published an economic assessment of configuration analysed [63].

The above results are numerically illustrated in Table 4 where the comparison for the same amount of freshwater produced is made. For the reasons indicated above, the maximum-time complementarity criterion is not presented. As can be seen, achieving the minimum unit cost implies reducing the size of the SWRO plant despite the need for a larger PV generator. In fact, this increase also implies a greater amount of energy not usable by the plant for desalination, which is around 10% more than for the criterion of minimum unusable energy.

Conclusions

Analyses conducted within the framework of this paper proves that off-grid SWRO desalination powered by hybrid tidal/PV systems in a favorable location achieves actual water production of one half of

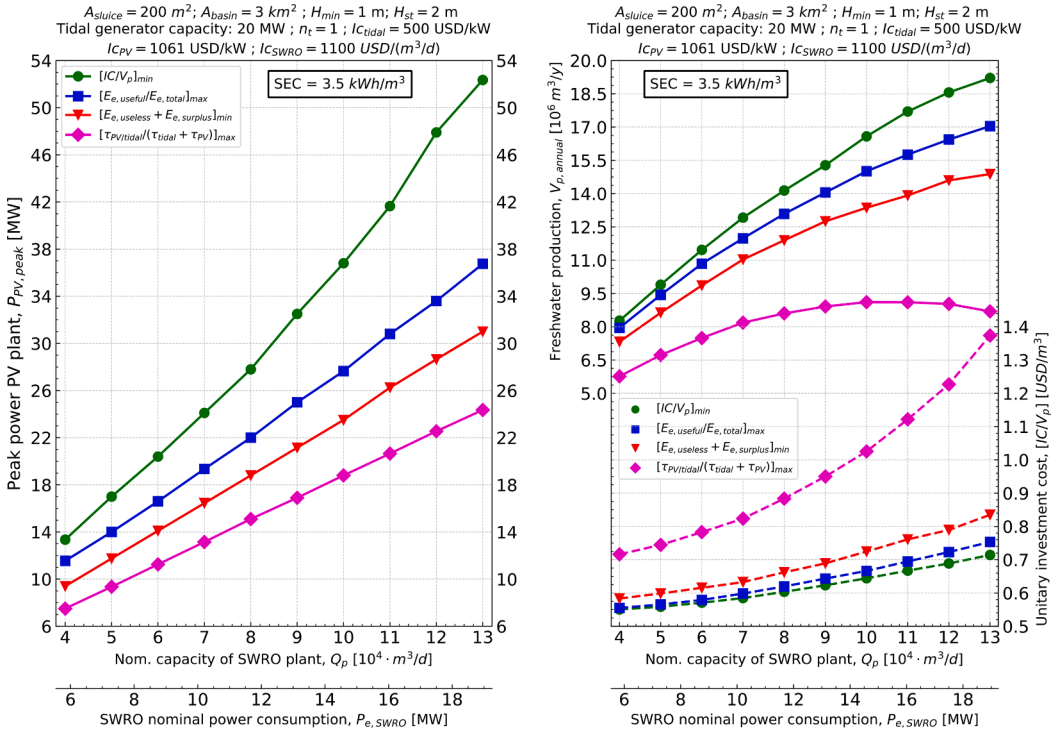

Fig. 16. a) solar PV sizes and b) yearly freshwater production and unitary investment cost under the optimization criteria considered.

Table 4
Design selection for three different design criteria.

SEC [kWh/m^3]	3,5			4,8		
Water production, $V_{p,annual}$ [10^6 m^3/y]	8,5			8,5		
Design criterion	Min. ($E_{e,useless} + E_{e,surplus}$)	Max. ($E_{e,useful}/E_{e,total}$)	Min. (IC/V_p)	Min. ($E_{e,useless} + E_{e,surplus}$)	Max. ($E_{e,useful}/E_{e,total}$)	Min. (IC/V_p)
Nominal SWRO capacity [m^3/d]	48,600	43,700	41,400	56,300	49,100	45,900
Nominal desalination consumption [MW]	7,09	6,37	6,04	11,26	9,82	9,18
PV generator [MW]	11,45	12,35	13,85	18,15	18,55	20,05
Total energy output [GWh/y]	66,3	67,9	70,6	78,2	78,9	82
Power availability factor,	48,0%	53,3%	56,3%	41,4%	47,5%	50,8%
Useful energy output [GWh/y]	29,8	29,8	29,8	40,8	40,8	40,8
Surplus energy [GWh/y]	27,4	31,9	35,8	19,7	25,9	30,9
Useless energy [GWh/y]	9,1	6,2	4,9	17,7	12,2	9,9
Unuseful energy [GWh/y]	36,5	38,1	40,8	37,4	38,1	40,8
Unitary investment cost 15 y - [USD/m^3]	0,59	0,56	0,55	0,71	0,66	0,64

nominal production with adequate selection of design parameters.

At Broome, the energy production of 20 MW of tidal range plant is similar to that of 25 MWp of solar PV plant. Table 3 summarizes the most relevant parameters concerning the preliminary design of a desalination system based on 20 MW of tidal power installed. Moreover, Fig. 15 allow to find designs with minimum (IC/V_p) for a given annual water demand as a function of the nominal power of the desalination plant for each tidal turbine of 20 MW of rated power. Besides, Fig. 14 depicts recommended designs referred to a 20 MW tidal range turbine. As an exemplary case, considering 12 MW of nominal desalination consumption for 20 MW of tidal generator, it brings a minimum investment cost per m^3 produced corresponding to a value of $P_{PV,peak}$ that slightly depends on SEC. This minimum is reached at $P_{PV,peak}$ of 26.9 MW and 24.9 MW for respective SEC values of 3.5 kWh/m^3 and 4.8 kWh/m^3. Respective values of unitary investment costs are 0.67 USD/m^3 and 0.76 USD/m^3. Obviously, the lower the efficiency of the SWRO plant, the higher the unitary investment cost because less fresh water is produced by the hybrid desalination system: 14.1 $\times$ 10^6 m^3/y for a SEC of 3.5 kWh/m^3 and 10x10^6 m^3/y if SEC is 4.8 kWh/m^3.

In addition to the economic point of view, other useful design criteria based on operating parameters have been analysed in order to show a holistic description of the system design. Power availability factor, surplus, useless and useful energy outputs of the system have been analysed as a function of the size of the solar PV generator and the nominal power consumption of the SWRO plant. The analysis performed confirms that the maximum ($E_{e,useful}/E_{e,total}$) is a suitable design criterion if a thorough cost assessment is not possible. In order to generalize this recommended criterion to any plant location, the corresponding assessment should be carried out covering a number of locations.

Expected range of investment costs of this technology in favorable locations are assessed per m^3 of water production considering that the desalination plant only operates at full capacity. Estimations of water costs require a case-by-case analysis based on considering the specific scenario of energy resources, economic and financial parameters along with optimized design and operation strategy of the desalination plant, which is out of the aim of this paper.

CRediT authorship contribution statement

Agustín M. Delgado-Torres: Conceptualization, Methodology, Software, Writing – review & editing, Visualization. **Lourdes García-Rodríguez:** Conceptualization, Writing – original draft, Writing – review & editing, Supervision, Funding acquisition.

Declaration of Competing Interest

The authors declare that they have no known competing financial interests or personal relationships that could have appeared to influence the work reported in this paper.

Acknowledgements

L. García-Rodríguez wishes to thank the European Regional Development Fund, Interreg Atlantic Area, for its financial assistance within the framework of the EERES4WATER Project (Second Call, Priority 2, EAPA_1058/2018). The University of Seville is also gratefully acknowledged for supporting this research through its Internal Research Programme (Plan Propio de Investigación), under contract No 2019/00000359.

References

[1] Crerar AJ, Pritchard C. Wave powered desalination: Experimental and mathematical modelling. Desalination 1991;81(1–3):391–8. https://doi.org/10.1016/0011-9164(91)85071-2.
[2] Crerar AJ, Low RE, Pritchard CL. Wave powered desalination. Desalination 1987;67:127–37. https://doi.org/10.1016/0011-9164(87)90238-4.
[3] Hicks DC, Mitcheson GR, Pleass CM, Salevan JF. Delbouy: Ocean wave-powered seawater reverse osmosis desalination systems. Desalination 1989;73:81–94. https://doi.org/10.1016/0011-9164(89)87006-7.
[4] García-Rodríguez L. Seawater desalination driven by renewable energies: A review. Desalination 2002;143(2):103–13. https://doi.org/10.1016/S0011-9164(02)00232-1.
[5] Bundschuh J, Kaczmarczyk M, Ghaffour N, Tomaszewska B. State-of-the-art of renewable energy sources used in water desalination: Present and future prospects. Desalination 2021;508:115035. https://doi.org/10.1016/j.desal.2021.115035.
[6] Ling C, Wang Y, Min C, Zhang Y. Economic evaluation of reverse osmosis desalination system coupled with tidal energy. Front Energy 2018;12(2):297–304.
[7] Resolute Marine Energy. Wave2O™ - Solar Impulse Efficient Solution. https://solarimpulse.com/solutions-explorer/wave2o ; 2022 [accessed 5 January 2022].
[8] Yang Y, Ji P, Zeng X, Fang J, Wu J. A Low Speed Piston Pump Directly Driven by Tidal Current Energy for Reverse Osmosis Desalination. Hsi-An Chiao Tung Ta Hsueh/J Xi'an Jiaotong Univers 2020;54(4):27–34. https://doi.org/10.7652/xjtuxb202004004.
[9] Greco F, Jarquìn-Laguna A. Simulation of a horizontal axis tidal turbine for direct driven reverse-osmosis desalination. Advances in Renewable Energies Offshore -. In: Proceedings of the 3rd International Conference on Renewable Energies Offshore; 2018. p. 181–8.
[10] Chen M-F, Zhang M-Y, Ling C-M. Computational Model for Performance Analysis of Direct-driven Tidal Energy Reverse Osmosis Seawater Desalination System. Kung Cheng Je Wu Li Hsueh Pao/J Eng Thermophys 2019;40(6):1211–8.
[11] Ling, C., Lou, X., Li, J., Zhang, Y. Experimental investigation of a novel tidal supercharger driven by tidal energy for reverse osmosis seawater desalination. Advances in Renewable Energies Offshore - Proceedings of the 3rd International Conference on Renewable Energies Offshore, RENEW 2018; 2019:191-194.
[12] Zhao G, Su X, Cao Y, Su J, Liu Y. Experiments on the hydrodynamic performance of horizontal axis tidal current turbine and desalination of sea water. Int J Energy Res 2016;40(5):600–9. https://doi.org/10.1002/er.3442.
[13] Delgado-Torres AM, García-Rodríguez L, del Moral MJ. Preliminary assessment of innovative seawater reverse osmosis (SWRO) desalination powered by a hybrid solar photovoltaic (PV) - Tidal range energy system. Desalination 2020;477:114247. https://doi.org/10.1016/j.desal.2019.114247.
[14] Delgado-Torres, A.M., García-Rodríguez, L. Desalination powered by hybrid solar photovoltaic (PV) and tidal range energy systems – Future Prospects. In: Gude, V.G. (Eds.). Energy Storage for Multi-generation: Desalination, power, cooling and heating applications, Elsevier; 2022 (Accepted).
[15] Li Z, Siddiqi A, Anadon LD, Narayanamurti V. Towards sustainability in water-energy nexus: Ocean energy for seawater desalination. Renew Sustain Energy Rev 2018;82:3833–47. https://doi.org/10.1016/j.rser.2017.10.087.
[16] IRENA International Renewable Energy Agency, Renewable power generation costs in 2020. https://www.irena.org/publications/2021/Jun/Renewable-Power-Costs-in-2020 ; 2020 [accessed 7 January 2022].

[17] Xue J, Ahmadian R, Jones O. Genetic Algorithm in Tidal Range Schemes' Optimisation. Energy 2020;200:117496. https://doi.org/10.1016/j.energy.2020.117496.
[18] WorldTides - Tide predictions for any location in the worldTides - Tide predictions for any location in the world https://www.worldtides.info/?latlon=56.533298,-61.683300 ; 2021 [accessed 3 April 2022].
[19] Tidal Repository - Tidal Software. https://www.tidalsoftware.com/solutions/tidal-repository/. [accessed 3 April 2022].
[20] Simon P. Neill, Athanasios Angeloudis, Peter E. Robins, Ian Walkington, Sophie L. Ward, Ian Masters, Matt J. Lewis, Marco Piano, Alexandros Avdis, Matthew D. Piggott, George Aggidis, Paul Evans, Thomas A.A. Adcock, Audrius Zidonis, Reza Ahmadian, Roger Falconer. Tidal range energy resource and optimization e Past perspectives and future challenges. Renewable Energy 2018; 127:763-778. Doi: 10.1016/j.renene.2018.05.007 0960-1481.
[21] Kim JW, Ha HK, Woo SB. Dynamics of sediment disturbance by periodic artificial discharges from the world's largest tidal power plant. Estuar Coast Shelf Sci 2017; 190:69–79. https://doi.org/10.1016/j.ecss.2017.03.029.
[22] Stuyfzand PJ, Joost, Kappelhof WNM. Floating, high-capacity desalting islands on renewable multi-energy supply. Desalination 2005;177(1–3):259–66. https://doi.org/10.1016/j.desal.2004.12.011.
[23] Obara S, Morizane Y, Morel J. Study on method of electricity and heat storage planning based on energy demand and tidal flow velocity forecasts for a tidal microgrid. Appl Energy 2013;111:358–73. https://doi.org/10.1016/j.apenergy.2013.05.018.
[24] Sheng L, Zhou Z, Charpentier JF, Benbouzid MEH. Stand-alone island daily power management using a tidal turbine farm and an ocean compressed air energy storage system. Renewable Energy 2017;103:286–94. https://doi.org/10.1016/j.renene.2016.11.042.
[25] Manchester S, Barzegar B, Swan L, Groulx D. Energy storage requirements for in-stream tidal generation on a limited capacity electricity grid. Energy 2013;61: 283–90. https://doi.org/10.1016/j.energy.2013.08.036.
[26] Ioannis Kougias, George Aggidis, François Avellan, Sabri Deniz, Urban Lundin, Alberto Moro, Sebastian Muntean, Daniele Novara, Juan Ignacio Pérez-Díaz, Emanuele Quaranta, Philippe Schild, Nicolaos Theodossiou, Analysis of emerging technologies in the hydropower sector. Renew Sustain Energy Rev 2019;113: 109257, Doi: 10.1016/j.rser.2019.109257.
[27] Naderipour A, Abdul-Malek Z, Nowdeh SA, Kamyab H, Ramtin AR, Shahrokhi S, et al. Comparative evaluation of hybrid photovoltaic, wind, tidal and fuel cell clean system design for different regions with remote application considering cost. J Cleaner Prod 2021;283:124207.
[28] Kucukali S. Finding the most suitable existing hydropower reservoirs for the development of pumped-storage schemes: An integrated approach. Renew Sustain Energy Rev 2014;37:502–8.
[29] Loisel R, Sanchez-Angulo M, Schoefs F, Gaillard A. Integration of tidal range energy with undersea pumped storage. Renewable Energy 2018;126:38–48. https://doi.org/10.1016/j.renene.2018.03.037.
[30] Gude VG. Energy Storage for Desalination. In: Gude VG, editor. Renewable Energy Powered Desalination Handbook: Application and Thermodynamics. Butterworth-Heinemann; 2018. p. 377–414. https://doi.org/10.1016/B978-0-12-815244-7.00010-6.
[31] Zakeri B, Syri S. Electrical energy storage systems: A comparative life cycle cost analysis. Renew Sustain Energy Rev 2015;42:569–96. https://doi.org/10.1016/j.rser.2014.10.011.
[32] Mejia-Olivares CJ, Haigh ID, Angeloudis A, Lewis MJ, Neill SP. Tidal range energy resource assessment of the Gulf of California. Mexico Renew Energy 2020;155: 469–83. https://doi.org/10.1016/j.renene.2020.03.086.
[33] de Andres A, MacGillivray A, Roberts O, Guanche R, Jeffrey H. Beyond LCOE: A study of ocean energy technology development and deployment attractiveness. Sustainable Energy Technol Assess 2017;19:1–16. https://doi.org/10.1016/j.seta.2016.11.001.
[34] Angeloudis A, Kramer SC, Hawkins N, Piggott MD. On the potential of linked-basin tidal power plants: An operational and coastal modelling assessment. Renew Energy 2020;155:876–88. https://doi.org/10.1016/j.renene.2020.03.167.
[35] Recalde AA, Alvarez-Alvarado MS. Design optimization for reliability improvement in microgrids with wind – tidal – photovoltaic generation. Electr Power Syst Res 2020;188:106540. https://doi.org/10.1016/j.epsr.2020.106540.
[36] Quaranta E, Bahreini A, Riasi A, Revelli R. The Very Low Head Turbine for hydropower generation in existing hydraulic infrastructures: State of the art and future challenges. Sustainable Energy Technol Assess 2022;51:101924. https://doi.org/10.1016/j.seta.2021.101924.
[37] Hand BP, Erdogan N, Murray D, Cronin P, Doran J, Murphy J. Experimental testing on the influence of shaft rotary lip seal misalignment for a marine hydro-kinetic turbine. Sustainable Energy Technol Assess 2022;50:101874.
[38] Zhang J, Zhou Y, Lin X, Wang G, Guo Y, Chen H. Experimental investigation on wake and thrust characteristics of a twin-rotor horizontal axis tidal stream turbine. Renewable Energy 2022. https://doi.org/10.1016/j.renene.2022.05.061.
[39] Eng Jet Yeo, David M. Kennedy, Fergal O'Rourke, Tidal current turbine blade optimisation with improved blade element momentum theory and a non-dominated sorting genetic algorithm, Energy; 250, 2022, 123720, Doi: 10.1016/j.energy.2022.123720.
[40] Sun Ke, Yi Y, Zhang J, Zhang J, Zaidi SSH, Sun S. Influence of blade numbers on start-up performance of vertical axis tidal current turbines. Ocean Eng 2022;243: 110314. https://doi.org/10.1016/j.oceaneng.2021.110314.
[41] Sun ZhaoCheng, Li D, Mao YuFeng, Feng L, Zhang Y, Liu C. Anti-cavitation optimal design and experimental research on tidal turbines based on improved inverse BEM. Energy 2022;239:122263.
[42] Peng B, Zhang Y, Zheng Y, Wang R, Fernandez-Rodriguez E, Tang Q, et al. The effects of surge motion on the dynamics and wake characteristics of a floating tidal stream turbine under free surface condition. Energy Convers Manage 2022;266: 115816. https://doi.org/10.1016/j.enconman.2022.115816.
[43] Maldar NR, Ng CY, Patel MS, Oguz E. Potential and prospects of hydrokinetic energy in Malaysia: A review. Sustainable Energy Technol Assess 2022;52:102265.
[44] Goh H-B, Lai S-H, Jameel M, Teh H-M, Chin R-J. Feasibility assessment of tidal energy extraction at the Tg Tuan coastal headland: A numerical simulation study. Sustainable Energy Technol Assess 2020;38:100633. https://doi.org/10.1016/j.seta.2020.100633.
[45] Moore T, Boyle C. The tidal energy potential of the Manukau Harbour, New Zealand. Sustain Energy Technol Assessm 2014;8:66–73. https://doi.org/10.1016/j.seta.2014.07.001.
[46] Mutsuda H, Rahmawati S, Taniguchi N, Nakashima T, Doi Y. Harvesting ocean energy with a small-scale tidal-current turbine and fish aggregating device in the Indonesian Archipelagos. Sustainable Energy Technol Assess 2019;35:160–71. https://doi.org/10.1016/j.seta.2019.07.001.
[47] Soleimani K, Ketabdari MJ, Khorasani F. Feasibility study on tidal and wave energy conversion in Iranian seas. Sustainable Energy Technol Assess 2015;11:77–86.
[48] Bennis A-C, Furgerot L, Bailly Du Bois P, Poizot E, Méar Y, Dumas F. A winter storm in Alderney Race: Impacts of 3D wave–current interactions on the hydrodynamic and tidal stream energy. Appl Ocean Res 2022;120:103009. https://doi.org/10.1016/j.apor.2021.103009.
[49] Li Q, Venugopal V, Barltrop N. Modelling dynamic loadings of a tidal stream turbine in combined -urrent-turbulence environment. Sustainable Energy Technol Assess 2022;50:101795. https://doi.org/10.1016/j.seta.2021.101795.
[50] Li M, Cao S, Zhu X, Yang Xu. Techno-economic analysis of the transition towards the large-scale hybrid wind-tidal supported coastal zero-energy communities. Appl Energy 2022;316:119118. https://doi.org/10.1016/j.apenergy.2022.119118.
[51] Khanjanpour MH, Javadi AA. Optimization of a Horizontal Axis Tidal (HAT) turbine for powering a Reverse Osmosis (RO) desalination system using Computational Fluid Dynamics (CFD) and Taguchi method. Energy Convers Manage 2021;231:113833.
[52] Hossein Shahbeig, Alireza Shafizadeh, Marc A. Rosen and Bert F. Sels Exergy sustainability analysis of biomass gasification: a critical review. Biofuel Res J, 9(1), Serial Number 1, 2022, pp. 1592-1607. DOI: 10.18331/BRJ2022.9.1.5.
[53] Mohammad Mahdi Ahmadi, Alireza Keyhani, Soteris A. Kalogirou, Su Shiung Lam, Wanxi Peng, Meisam Tabatabaei, Mortaza Aghbashlo, Net-zero exergoeconomic and exergoenvironmental building as new concepts for developing sustainable built environments, Energy Convers Manage, 244, 2021, 114418, https://doi.org/10.1016/j.enconman.2021.114418.
[54] Rahnama E, Aghbashlo M, Tabatabaei M, Khanali M, Rosen MA. Spatio-temporal solar exergoeconomic and exergoenvironmental maps for photovoltaic systems. Energy Convers Manage 2019;195:701–11. https://doi.org/10.1016/j.enconman.2019.05.051.
[55] NREL, (n.d.). https://sam.nrel.gov/ ; [accessed 1 June 2019].
[56] Angeloudis A, Falconer RA. Sensitivity of tidal lagoon and barrage hydrodynamic impacts and energy outputs to operational characteristics. Renew Energy 2017; 114:337–51. https://doi.org/10.1016/j.renene.2016.08.033.
[57] Song S, Demirel YK, Atlar M, Shi W. Prediction of the fouling penalty on the tidal turbine performance and development of its mitigation measures. Appl Energy 2020;276:115498. https://doi.org/10.1016/j.apenergy.2020.115498.
[58] Ewing F, Thies PR, Shek J, Ferreira CB. Probabilistic failure rate model of a tidal turbine pitch system. Renew Energy 2020;160:987–97. https://doi.org/10.1016/j.renene.2020.06.142.
[59] Energy Plus, (n.d.). https://energyplus.net/weather ; [accessed 23 July 23 2019].
[60] Heihsel M, Lenzen M, Malik A, Geschke A. The carbon footprint of desalination: An input-output analysis of seawater reverse osmosis desalination in Australia for 2005–2015. Desalination 2019;454:71–81. https://doi.org/10.1016/j.desal.2018.12.008.
[61] IRENA International Renewable Energy Agency. Tidal energy. Technology Brief, 2014. https://www.irena.org/-/media/Files/IRENA/Agency/Publication/2014/Tidal_Energy_V4_WEB.pdf [accessed 7 January 2022].
[62] Subiela VJ, Peñate B, García-Rodríguez L. Configurations of reverse osmosis with variable energy consumption for off-grid wind-powered seawater desalination: system modelling and water cost. Desalin Water Treat 2020;180:1–15. https://doi.org/10.5004/dwt.2020.24991.
[63] Subiela VJ, Peñate B, García-Rodríguez L. Design recommendations and cost assessment for off-grid wind powered-seawater reverse osmosis desalination with medium-size capacity. Desalin Water Treat 2020;180:16–36. https://doi.org/10.5004/dwt.2020.25013.